Defense Nuclear Agency
Alexandria, VA 22310-3398

DNA-TR-95-55

ACE 4 Optimization Program

William Rix, et al.
Maxwell Labs
8888 Balboa Ave., Bldg. 1
San Diego, CA 92123

October 1996

Technical Report

19961029 061

CONTRACT No. DNA 001-92-C-0154

Approved for public release;
distribution is unlimited.

DTIC QUALITY INSPECTED 1

DESTRUCTION NOTICE:

Destroy this report when it is no longer needed.
Do not return to sender.

PLEASE NOTIFY THE DEFENSE SPECIAL WEAPONS AGENCY, ATTN: CSTI, 6801TELEGRAPH ROAD, ALEXANDRIA, VA 22310-3398, IF YOUR ADDRESS IS INCORRECT, IF YOU WISH IT DELETED FROM THE DISTRIBUTION LIST, OR IF THE ADDRESSEE IS NO LONGER EMPLOYED BY YOUR ORGANIZATION.

DISTRIBUTION LIST UPDATE

This mailer is provided to enable DSWA to maintain current distribution lists for reports. (We would appreciate your providing the requested information.)

NOTE:
Please return the mailing label from the document so that any additions, changes, corrections or deletions can be made easily. For distribution cancellation or more information call DSWA/IMAS (703) 325-1036.

☐ Add the individual listed to your distribution list.

☐ Delete the cited organization/individual.

☐ Change of address.

NAME: _____

ORGANIZATION: _____

OLD ADDRESS	CURRENT ADDRESS
_____	_____
_____	_____
_____	_____

TELEPHONE NUMBER: ( ) _____

DSWA PUBLICATION NUMBER/TITLE	CHANGES/DELETIONS/ADDITIONS, etc.) *(Attach Sheet if more Space is Required)*
_____	_____
_____	_____
_____	_____

DSWA OR OTHER GOVERNMENT CONTRACT NUMBER: _____

CERTIFICATION OF NEED-TO-KNOW BY GOVERNMENT SPONSOR (if other than DSWA):

SPONSORING ORGANIZATION: _____

CONTRACTING OFFICER OR REPRESENTATIVE: _____

SIGNATURE: _____

CUT HERE AND RETURN

DEFENSE SPECIAL WEAPONS AGENCY
ATTN: IMAS
6801 TELEGRAPH ROAD
ALEXANDRIA, VA 22310-3398

DEFENSE SPECIAL WEAPONS AGENCY
ATTN: IMAS
6801 TELEGRAPH ROAD
ALEXANDRIA, VA 22310-3398

REPORT DOCUMENTATION PAGE

Form Approved
OMB No. 0704-0188

Public reporting burden for this collection of information is estimated to average 1 hour per response including the time for reviewing instructions, searching existing data sources, gathering and maintaining the data needed, and completing and reviewing the collection of information. Send comments regarding this burden estimate or any other aspect of this collection of information, including suggestions for reducing this burden, to Washington Headquarters Services Directorate for information Operations and Reports, 1215 Jefferson Davis Highway, Suite 1204, Arlington, VA 22202-4302, and to the Office of Management and Budget, Paperwork Reduction Project (0704-0188), Washington, DC 20503.

1. AGENCY USE ONLY (Leave blank)	2. REPORT DATE	3. REPORT TYPE AND DATES COVERED
	961001	Technical 921808 – 943001

4. TITLE AND SUBTITLE

ACE 4 Optimization Program

5. FUNDING NUMBERS

C - DNA 001-92-C-0154
PE - 62715H
PR - AB
TA - GE
WU - DH326720

6. AUTHOR(S)

William Rix, John Thompson, A. Richard Miller, Daniel Husovsky and Eduardo Waisman

7. PERFORMING ORGANIZATION NAME(S) AND ADDRESS(ES)

Maxwell Labs
8888 Balboa Ave., Bldg. 1
San Diego, CA 92123

8. PERFORMING ORGANIZATION REPORT NUMBER

MLR-4338

9. SPONSORING/MONITORING AGENCY NAME(S) AND ADDRESS(ES)

Defense Special Weapons Agency
6801 Telegraph Road
Alexandria, VA 22310-3398
RAST/Filios

10. SPONSORING/MONITORING AGENCY REPORT NUMBER

DNA-TR-95-55

11. SUPPLEMENTARY NOTES

This work was sponsored by the Defense Special Weapons Agency under RDT&E RMC Code B4662D AB GE 00003 3300A 25904D.

12a. DISTRIBUTION/AVAILABILITY STATEMENT

Approved for public release; distribution is unlimited.

12b. DISTRIBUTION CODE

13. ABSTRACT (*Maximum 200 words*)

Previous DNA contracts developed the ACE 4 quarter-scale DECADE prototype. The ACE 4 opening switch required optimization.

This effort was in two phases: Phase 1, plasma source optimization and Phase 2, ACE 4 switch optimization. Phase 1 included development of a slow flashboard plasma source and a multi-channel laser interferometer to measure the density and uniformity produced by the old flashboards and a 1/5 scale version of the new plasma source. Phase 1 schedule and technical goals were met as indicated below:

	Goal	Achieved
Schedule	180 days after contract issue	185 days after contract issue
Plasma Source Density	2×10^{15} electrons/cm^3	3.8×10^{15} electrons/cm^3
Plasma Source Uniformity	$\sigma < \pm 30\%$	$\sigma = \pm 10\%$

14. SUBJECT TERMS

ACE 4
Plasma Opening Switch
Flashboard Plasma Source
Plasma Source Characterization

15. NUMBER OF PAGES

38

16. PRICE CODE

17. SECURITY CLASSIFICATION OF REPORT	18. SECURITY CLASSIFICATION OF THIS PAGE	19. SECURITY CLASSIFICATION OF ABSTRACT	20. LIMITATION OF ABSTRACT
UNCLASSIFIED	UNCLASSIFIED	UNCLASSIFIED	SAR

NSN 7540-280-5500

Standard Form 298 (Rev.2-89)
Prescribed by ANSI Sts. 239-18
298-102

CLASSIFIED BY:

N/A since Unclassified.

DECLASSIFY ON:

N/A since Unclassified.

13. ABSTRACT (Continued).

For Phase 2 performance into both short-circuit and e-beam diode loads was optimized with the new plasma source. The goals and the results were:

	Goal	Achieved
POS Short-Circuit Current	> 6 MA	8 MA
E-Beam Voltage	> 900 kV	300 kV
E-Beam Current	> 5 MA	2 MA
10-90% Current Rise into E-beam	< 70 ns	80 ns

ACE 4 POS operation into short-circuit loads exceeded the goal. However the POS didn't generate enough impedance to achieve the goals for an e-beam diode load.

CONVERSION TABLE

Conversion factors for U.S. Customary to metric (SI) units of measurement.

MULTIPLY → / TO GET ←	BY → / BY ←	TO GET / DIVIDE
angstrom	meters (m)	1.000 000 x E -10
atmosphere (normal)	kilo pascal (kPa)	1.013 25 x E +2
bar	kilo pascal (kPa)	1.000 000 x E +2
barn	meter^2 (m^2)	1.000 000 x E -28
British thermal unit (thermochemical)	joule (J)	1.054 350 x E +3
cal (thermochemical)/cm^2	mega joule/m^2 (MJ/m^2)	4.184 000 x E -2
calorie (thermochemical)	joule (J)	4.184 000
calorie (thermochemical)/g	joule per kilogram (J/kg)*	4.184 000 x E +3
curies	gig becquerel (Gbq)+	3.700 000 x E +1
degree Celsius	degree kelvin (K)	$t_K = t°_C = 273.15$
degree (angle)	radian (rad)	1.745 329 x E -2
degree Fahrenheit	degree kelvin (K)	$t_K = (t°_F + 459.67)/1.8$
electron volt	joule (J)	1.602 19 x E -19
erg	joule (J)	1.000 000 x E -7
erg/second	watt (W)	1.000 000 x E -7
foot	meter (m)	3.048 000 x E -1
foot-pound-force	joule (J)	1.355 818
gallon (U.S. liquid)	meter^3 (m^3)	3.785 412 x E -3
inch	meter (m)	2.540 000 x E -2
jerk	joule (J)	1.000 000 x E +9
joule kilogram (J/kg) (radiation dose absorbed)	gray (Gy)*	1.000 000
kilotons	terajoules	4.183
kip (1000 lbf)	newton (N)	4.448 222 x E +3
kip/inch^2 (ksi)	kilo pascal (kPa)	6.894 757 x E +3
ktap	newton-second/m^2 (N-s/m^2)	1.000 000 x E +2
micron	meter (m)	1.000 000 x E -6
mil	meter (m)	2.540 000 x E -5
mile (international)	meter (m)	1.609 344 x E +3
ounce	kilogram (kg)	2.834 952 x E -2
pound-force (lbf avoirdupois)	newton (N)	4.488 222
pound-force inch	newton-meter (N•m)	1.129 848 x E -1
pound-force/inch	newton/meter (N•m)	1.751 268 x E +2
pound-force/foot^2	kilo pascal (kPa)	4.788 026 x E -2
pound-force/inch^2 (psi)	kilo pascal (kPa)	6.894 757
pound-mass (lbm avoirdupois)	kilogram (kg)	4.535 9024 x E -1
rad (radiation dose absorbed)§	gray (Gy)*	1.000 000 x E -2
roentgen§	coulomb/kilogram (C/kg)	2.579 760 x E -4
shake	second (s)	1.000 000 x E -8
slug	kilogram (kg)	1.459 390 x E -1
torr (mm Hg, O• C)	kilo pascal (kPa)	1.333 22 x E -1

* The gray (Gy) is the accepted SI unit equivalent to the energy imparted by ionizing radiation to a mass and corresponds to one joule/kilogram.

\+ The becquerel (Bq) is the SI unit of radioactivity; 1 Bq = 1 event/s.

TABLE OF CONTENTS

FIGURES

SECTION 1
OVERVIEW

1.1 BACKGROUND.

Maxwell Laboratories has provided research and development in the area of pulsed power for nuclear weapons effects simulators for many years. These efforts are aimed at providing a high-fidelity nuclear weapon effects environment for hardness and survivability testing of electronics and optical systems. Previous DNA contracts (DNA001-88-C-0138 and DNA001-88-C-0141) developed and tested a quarter-scale prototype for DNA's DECADE simulator program. This prototype, ACE 4, required optimization of its opening switch in order to evaluate its efficacy for use as an operational test facility.

1.2 STATEMENT OF WORK.

This effort was structured as a two phase program. Commencement of the second phase was contingent on success in the first phase. Each phase of the program will now be described.

1.2.1 Phase 1. Plasma Source Optimization Demonstration.

The useful plasma density from the ACE 4 opening switch plasma source needed to be increased from the 1.5×10^{14} electrons/cm^3 level to 2×10^{15} electrons/cm^3. Part of this task involved documenting the plasma source performance by installing the required diagnostics and making measurements on ACE 4. After demonstration of a prototype, a full ACE 4 plasma source could then be designed and fabricated including upgraded pulsers and cable assemblies.

1.2.2 Phase 2. ACE 4 Switch Optimization.

In this phase the plasma source developed in Phase 1 was to be used to optimize ACE 4 plasma opening switch operation. The goals of this switch optimization were to conduct over 6 MA and then open at voltages above 900 kV and drive over 5 MA into an e-beam diode in less than 70 ns.

1.3 RESULTS.

Phase 1 technical work required the development of a new type of flashboard which we called a "slow" flashboard because we deliberately slowed down the velocity of the plasma relative to a conventional flashboard. As part of this task we developed a multi-channel laser interferometer which could be installed on ACE 4 to measure the density and uniformity of the plasma produced by both the old, conventional flashboards and a prototype, 1/5 scale version of a full ACE 4 plasma source. Phase 1 schedule and technical goals were met as indicated in the table below.

	Goal	Achieved
Schedule	180 days after contract issue	185 days after contract issue
Plasma Source Density	2×10^{15} electrons/cm^3	3.8×10^{15} electrons/cm^3
Plasma Source Uniformity	$\sigma < \pm 30\%$	$\sigma = \pm 10\%$

From the above it is clear that we were successful in meeting or exceeding our goals for the first phase of ACE 4 optimization. We proceeded to Phase 2.

For Phase 2 we were required to build and install a full-scale version of the prototype plasma source developed in Phase 1 and then optimize ACE 4 POS performance into both short-circuit and e-beam diode loads with the new plasma source. Phase 2 had no specified schedule requirement. The technical goals and the progress made in achieving the goals are indicated in the table below.

	Goal	Achieved
POS short-circuit current	> 6 MA	8 MA
E-beam voltage	> 900 kV	300 kV
E-beam current	> 5 MA	2 MA
10 to 90% current rise into e-beam	< 70 ns	80 ns

ACE 4 POS operation into short-circuit loads exceeded the goals by conducting more than the required current. However we did not achieve the goals for operation with an e-beam diode load. In simplest terms, the POS did not generate enough impedance to meet the goals. We based our design on theory and experimental evidence that indicates that as the plasma is snow-plowed down the length of the switch, the density is thinned out along a relatively narrow channel by the time the snow-plow reaches the end of the switch and the opening occurs across

this channel. Analysis of the ACE 4 optimization data indicated that with the new, higher density plasma source, opening did not occur at the physical end of the switch. We believe additional plasma diagnostics will indicate that the plasma did not thin out as rapidly as expected in ACE 4 and that the switch was unable to open fully before the plasma reached the load.

1.4 CONCLUSIONS AND RECOMMENDATIONS FOR FOLLOW-ON WORK.

This work resulted in significant progress in plasma source design for opening switches. We achieved impressive increases in density, uniformity, and durability. All of these attributes are essential for operation of high current, long conduction time opening switches. We also implemented plasma diagnostics on ACE 4 which make it possible to analyze and model switch operation and therefore approach plasma opening switch development in a scientific manner. Improved measurements can be combined with theory and modeling to understand how to increase the opened switch impedance. For follow-on work Maxwell is proposing performing additional experiments in which the initial plasma conditions are varied in a controlled manner. The data from these experiments could then be combined with modeling to suggest ways to improve opening switch capability for driving high impedance loads.

The following sections contain more detailed data and discussions of the tasks performed for this contract.

SECTION 2
BACKGROUND

2.1 THE ACE CONCEPT.

The current generation of nuclear weapon effects simulators (BLACKJACK 5, DOUBLE-EAGLE, and PHOENIX) uses capacitive energy storage and closing switch technology to achieve the power conditioning required for driving radiation producing loads. Capacitive storage and closing switch technology is extremely difficult and expensive to scale to simulators above the 25 TW level. A cost-effective and technically feasible alternative for power conditioning is to use inductive storage and opening switch technology.

The ACE concept uses only inductive storage and opening switches for power conditioning. A storage inductor is coupled to a fast opening switch to reduce the microsecond pulses generated by the capacitor bank to the 100 to 200 ns pulse widths required for driving imploding plasma radiation sources. ACE 4, shown in Figure 2-1, is a 4 MJ realization of the concept built by the Defense Nuclear Agency at Maxwell as a prototype for a DECADE simulator.

The ACE 4 pulse power design is very compact. Primary energy storage consists of 192 1.5 μF, ±90 kV capacitors configured in 24 Marx generators. Each Marx generator consists of four switched capacitor stages in series. The four capacitor stages each have two capacitors in parallel. Marx generators are stacked two high with three stacks (1 MJ) per Marx tank, in the four Marx tanks. Each stacked Marx pair drives a common output bus at the stack center. The top and bottom of the stack are grounded, so that the Marx pair is in parallel. Each Marx stack feeds a posthole convolute connection to two triplate oil transmission lines through a 0.125 mΩ damping resistor assembly. The 24 triplate oil transmission lines connect to the common load coupler through additional posthole convolutes. At the load coupler the power flow splits to separate top and bottom oil-vacuum interfaces which drive a radial triplate vacuum transmission line. This configuration is shown in Figure 2-2.

The key component in ACE 4 is the plasma opening switch (POS). The POS is located in the radial triplate region of the vacuum transmission line and provides the power conditioning. A top and bottom POS are coupled at their inputs through the parallel, vacuum interfaces as shown in Figure 2-3. The top and bottom POS drive a common load. Two sets of 40 flashboards each provide plasma for the top and bottom POS.

In the opening switch plasma source configuration operated in work performed under earlier contracts, each flashboard consisted of 5 gap-chains of 20 gaps in a conventional configuration. The flashboards were wedge shaped in order to fill the annular region facing the transparent anode. The annular aperture in the transparent anode, which defines the maximum POS area, extends from an inner diameter of 80 cm to an outer diameter of 128 cm.

2.2 ACE 4 PLASMA SOURCE LIMITED RESULTS.

ACE 4 initial performance was characterized with the conventional flashboard plasma source described above incorporated in the opening switch. With this plasma source, ACE 4 plasma formation time was limited to less than 1.75 μs due to deleterious effects of plasma spreading away from the switch at a velocity of 15 to 20 cm/μs. With 1.75 μs of plasma formation, only 4 to 5 MA could be conducted in the POS for a corresponding conduction time of 600 to 800 ns out of a quarter-period of 1.5 μs. In tests completed in April 1992 this configuration was shown to develop 450 kV into a load with the switch impedance being characterized by a dZ/dt of 1 to 2 x 10^6 Ω/s and a Z_{max} of about 0.1 to 0.2 Ω. Based on test-stand measurements made on conventional ACE 4 flashboards, the plasma density in the POS region during the conduction phase was estimated to be on the order of 10^{14} electrons/cm^3. Using the estimated density from the test-stand flashboard characterization in the S-Cubed model for the POS [1], [2] on ACE 4 produces good agreement with the experimental data as shown in the plots in Figure 2-4.

The S-Cubed POS model for ACE 4 indicated that increasing plasma density by a factor of 10 in the POS would increase the power available to a load from about 1 TW to over 5 TW. These predictions motivated DNA to investigate improved plasma sources for the opening switch.

SECTION 3
PHASE 1, PLASMA SOURCE OPTIMIZATION

3.1 CONVENTIONAL PLASMA SOURCES.

Numerous plasma sources have been tested for use in plasma opening switches. Initial experiments at NRL which first demonstrated power gain for plasma opening switches used cable gun sources. On Gamble II cable guns produced plasma densities of 10^{12} electrons/cm^3 and conducted about 1 MA for conduction times of about 100 ns. However scaling the cable gun sources to larger pulsed power generators like PBFA 2 or BLACKJACK 5 resulted in a requirement for an impracticably large number of cable sources. Flashboards offered an alternative for large areas and densities in the 10^{14} electron/cm^3 and above range. Flashboard plasma sources based initially on Sandia designs were developed for use on BLACKJACK 5 and the ACE series of inductive storage technology generators at Maxwell. Simple models of flashboard operation have been developed [3].

Details of the conventional flashboards used in the initial ACE 4 experiments conducted under previous DNA contracts are shown in Figure 3-1. The conventional flashboard face consists of five chains of copper electrodes etched onto a Kapton substrate. This face is mounted onto a G-10 backing plate with a ground plane sandwiched between the G-10 and the Kapton face. The flashboard generates plasma when a 20 to 30 kV pulse is placed across the electrode surfaces. The electrodes break down and the magnetic field confined between the ground plane and the conducting surface accelerate the plasma towards the switch region. Measurements indicate the plasma reaches velocities as high as 20 cm/μs.

3.2 SLOW FLASHBOARD CONCEPT.

The improved plasma source uses "slow" flashboards. The flashboard plasma is slowed by changing the current return geometry as indicated in Figure 3-2. Instead of returning through the ground plane, the current is routed through feed wires placed above the electrode gaps where the plasma is formed. The magnetic field associated with the feed wires inhibits the acceleration of the plasma away from the flashboard face. The slower plasma velocity from the flashboards of about 3 cm/μs allows plasma formation times of up to 10 μs before plasma spread into the vacuum power flow regions upstream and downstream of the switch becomes a problem. Figure 3-3 is a picture of a slow flashboard.

In addition to redesigning the flashboards, a significant effort was put into improving the pulsers, cables, and vacuum feedthroughs used to deliver power to the flashboards. During initial testing of ACE 4, breakdown problems in the cables and feedthroughs had significantly impacted the reproducibility and shot rate of the ACE 4 data. By applying standard pulse power engineering techniques to the experimentally revealed problems, significant improvements in performance, reliability, and reproducibility were achievable. Peak flashboard currents for this configurations was 8 kA per gap-chain.

3.3 PLASMA SOURCE CHARACTERIZATION AND ACCEPTANCE TEST PROCEDURES.

3.3.1 Test Configuration.

The characterization of the conventional flashboards used in the initial testing on ACE 4 and an acceptance test for the prototype of the slow flashboard plasma source were conducted in one quadrant of the upper half of the ACE 4 plasma opening switch. The one-fifth scale prototype of the full ACE 4 plasma source was large enough to produce density, uniformity, and reliability data which could be easily scaled to the full plasma source. In both cases the pulsers that provided power to the flashboards were operated at the nominal voltage. Figures 3-4 and 3-5 indicate the configurations used for the characterization of the conventional flashboards and the acceptance test of the slow flashboards, respectively.

3.3.2 Test Instrumentation.

The primary test instrument was a helium-neon laser interferometer for measuring the plasma electron density produced by the plasma source in the ACE 4 plasma opening switch. This instrument was developed as a part of the Statement of Work for this contract. Our instrument is based on a technique first used at NRL to measure plasma density in the POS [4]. The interferometry set-up consisted of five separate channels in order to acquire uniformity data at several sites on the same shot. The plasma path interferometer beams enter the ACE 4 vacuum chamber from the bottom and enter the POS region along the centerline. Turning mirrors direct the beams parallel to the flashboards along the middle of the anode-cathode (A-K) gap. The beams are reflected, and then retrace their paths back out of the vacuum vessel to rejoin the rest of the interferometer. A picture of the hardware assembled for the multi-channel interferometer is shown in Figure 3-6. Figure 3-7 , taken by blowing a small amount of smoke into the ACE 4

vacuum chamber, indicates the lines of sight for the interferometer in anode-cathode gap of the opening switch.

3.3.3 Test Procedure.

The time resolved plasma density and uniformity at mid-gap was measured for both the old plasma source system and for the optimized plasma source. For the conventional boards 5 channels of interferometry were used while for the slow boards, each shot produced 6 line density measurements. A total of 40 shots constituted each test and produced 200 and 240 measurements of line integrated density, respectively. To translate from line-integrated density to density, we used the length of the flashboard. If the prototype system performed perfectly, all 240 measurements would have been the same.

3.3.4 Results.

For the conventional flashboards, the average density at 1.75 μs formation time was 1.4 x 10^{14} electrons/cm^3 with a standard deviation of 16% over the 200 data points in the test series

An open shutter photograph of the slow flashboard array firing is pictured in Figure 3-8. At 5.55 μs of formation time, the average density was 3.8 x 10^{15} electrons/cm^3 with a standard deviation over the 240 data points of 10%. Typical density profiles in Figure 3-9 make clear the advantages of the improved plasma source.

The improved flashboards meet the optimized plasma source requirements. Usable density measured was about double the requirement in the Statement of Work and 20 times the pre-optimized capability. Uniformity measured was 3 time the requirement and 50% better than the pre-optimized capability. Reliability was demonstrated when each of the flashboards fired for 100 shots with no failures and less than 10% reduction in output density. The improved, slow plasma flashboards were deemed qualified to support ACE 4 optimization and DNA authorized proceeding with Phase 2 of the contract.

SECTION 4
PHASE 2, ACE 4 POS OPTIMIZATION

4.1 EXPERIMENTAL DESIGN CONSIDERATIONS.

The ACE 4 optimization approach was based on the idea that the physics of high plasma density POS operation during the conduction phase is dominated by hydrodynamic effects. This view is able to explain how a long conduction time, high density POS can open rapidly. Rapid opening requires that low plasma densities be present at the time of opening. If the initial plasma density distribution has the right profile across the gap, the current front develops a bow which pushes much of the plasma off to the sides, thinning the plasma in the region where a gap can be opened. How this can come about is shown in Figure 4-1, which gives the results of a simple two-dimensional snowplow calculation for an actual plasma source initial density distribution measured on ACE 4. In the case of the radial ACE 4 geometry where there is no magnetic field gradient across the gap, a minimum in the initial intergap density profile, as seen in Figure 4-1a, is required. Because of the intergap density minimum, the current front develops a bow, as shown in Figure 4-1b. Figure 4-1c show the thinning effect in terms of the modeled line integrated density along the direction of power flow. According to the model the integrated line density is reduced by an order of magnitude by the time the current front reaches the end of the POS. The actual density at the point of opening is a function of the physical length of the plasma front. This length has not been determined by either our simple snowplow models or our experimental measurements.

Our explanation for the low impedance generated by the initially tested fast flashboard plasma source is that it was unable to provide a plasma density distribution across the gap with a sufficiently deep minimum. This requirement on the density distribution is in addition to the requirement that the injected plasma reach a high enough average density in the switch region to conduct for the entire quarter-cycle before the plasma drifts into the transmission line between the switch and the load. In the compact ACE 4 radial geometry, with a load located typically 25 cm downstream, both considerations are crucial to proper operation the switch.

4.2 EXPERIMENTAL DATA AND INTERPRETATION.

The configuration used to test the new plasma source POS on ACE 4 in shown in Figure 4-2. For short-circuit load testing, a short-circuit was inserted between the e-beam anode and cathode. The new plasma source performed reliably and uniformly as projected from the prototype tests.

Good plasma uniformity, as evidenced by POS performance in terms of both azimuthal and top-to-bottom POS opening symmetry, is indicated in Figure 4-3 which shows the local current measurements about the azimuth just downstream of the physical POS for both the top and bottom POS.

Figures 4-4a and b show the results of ACE 4 shots using the slow plasma flashboard plasma source for both short circuit and e-beam loads. Conduction times approaching the ACE 4 quarter period were achieved with good top-to-bottom POS synchronization and opening times of about 150 ns. This data indicates we exceeded our goals for the short-circuit loads with the slow flashboard plasma source. Figure 4-4b, however, shows that the ability of the POS to drive a nominally 0.25 Ω e-beam diode was poor. The calculated POS impedance for these shots was about half that previously reported using fast plasma flashboards.[5] Interferometry measurements of this flashboard configuration indicated that the desired density profile was not achieved in the relatively short injection times required to keep the POS conduction time under the ACE 4 quarter period. In other words, the slow flashboards produced too much plasma.

The top POS flashboard plasma source was reconfigured to produce less plasma while maintaining the desired gap plasma distribution so that the conduction times could be kept under the ACE 4 quarter period. Figure 4-5 shows the results for a short circuit shot in this plasma source configuration. In this case opening was not as good as predicted. The reason may be related to plasma moving past the end of the switch. A significant time delay was observed between the outer current monitors just downstream of the POS region and the inner current monitors farthest downstream. Also, the current monitors farthest downstream did not show current transfer consistent with the inductively corrected POS voltage. The calculated relative inductance downstream of E-dot monitor as a function of time has been overlaid in Figure 3-3. During most of the conduction phase the inductance changes by approximately 6 nH, a value consistent with the POS region vacuum inductance. At the time that the outer cavity probes begin to come up, the inductance begins to increase more rapidly, and then plateaus shortly after the farthest downstream current monitor indicates current. The observed 10 nH change corresponds to 90 percent of the vacuum inductance downstream of the POS. This suggests that some portion of the POS plasma carrying the current across the anode-cathode gap was pushed beyond the end of the physical POS all the way to the short circuit load, 25 cm downstream. The observed POS voltage can be completely accounted for by plasma motion (IdL/dt) downstream of the physical POS.

Our modeling does not include the plasma profile or motion downstream of the POS, which may be a serious problem in the compact radial geometry of ACE 4. If sufficient thinning is not obtained by the end of the physical POS, switch opening may be affected by downstream geometry with the possibility of plasma motion for extended distances downstream.

4.3 CONCLUSIONS.

The slow plasma flashboard source was designed and tested on ACE 4. While the optimized slow plasma flashboard source was capable of conducting more than the desired 6 MA and of providing an intergap density profile which exhibited thinning during the conduction phase according to the snowplow model, it did not sufficiently localize the POS opening in the compact radial ACE 4 geometry to allow coupling to a load.

SECTION 5
REFERENCES

1 W. Rix, et al., "Operation and Empirical Modeling of the Plasma Opening Switch," (Unclassified) IEEE Transactions on Plasma Science, Vol. 19, 2, Apr. 1991. (Unclassified)

2 Parks, D., et al., "Mechanisms Affecting Long Conduction Time Plasma Opening Switches"(Unclassified), Applied Physics Letters, 59 (22), 25 Nov. 1991. (Unclassified)

3 D.G. Colombant and B.V. Weber, IEEE Transactions on Plasma Science, (Unclassified) Vol. PS-15, pp. 741-746, 1987. (Unclassified)

4 D.D. Hinshelwood, et. al., "Density Measurements of Microsecond-Conduction Time POS," (Unclassified) Beams 92 Proceedings, pp 603-608. (Unclassified)

5 W. Rix, et al., "Experiments on Microsecond Conduction Time Plasma Opening Switch Mechanisms," (Unclassified) Beams 92 Proceedings, pp 598-602. (Unclassified)

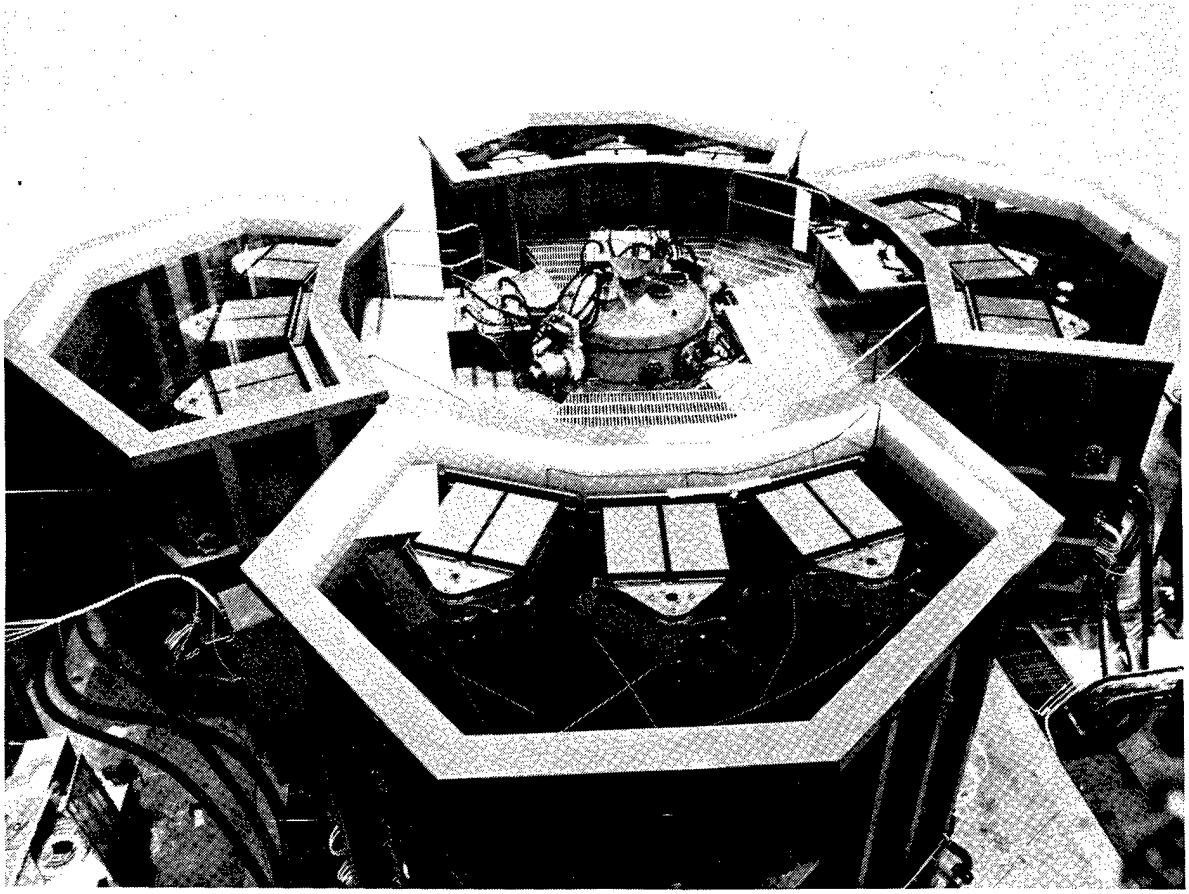

Figure 2-1. ACE 4 design is compact.

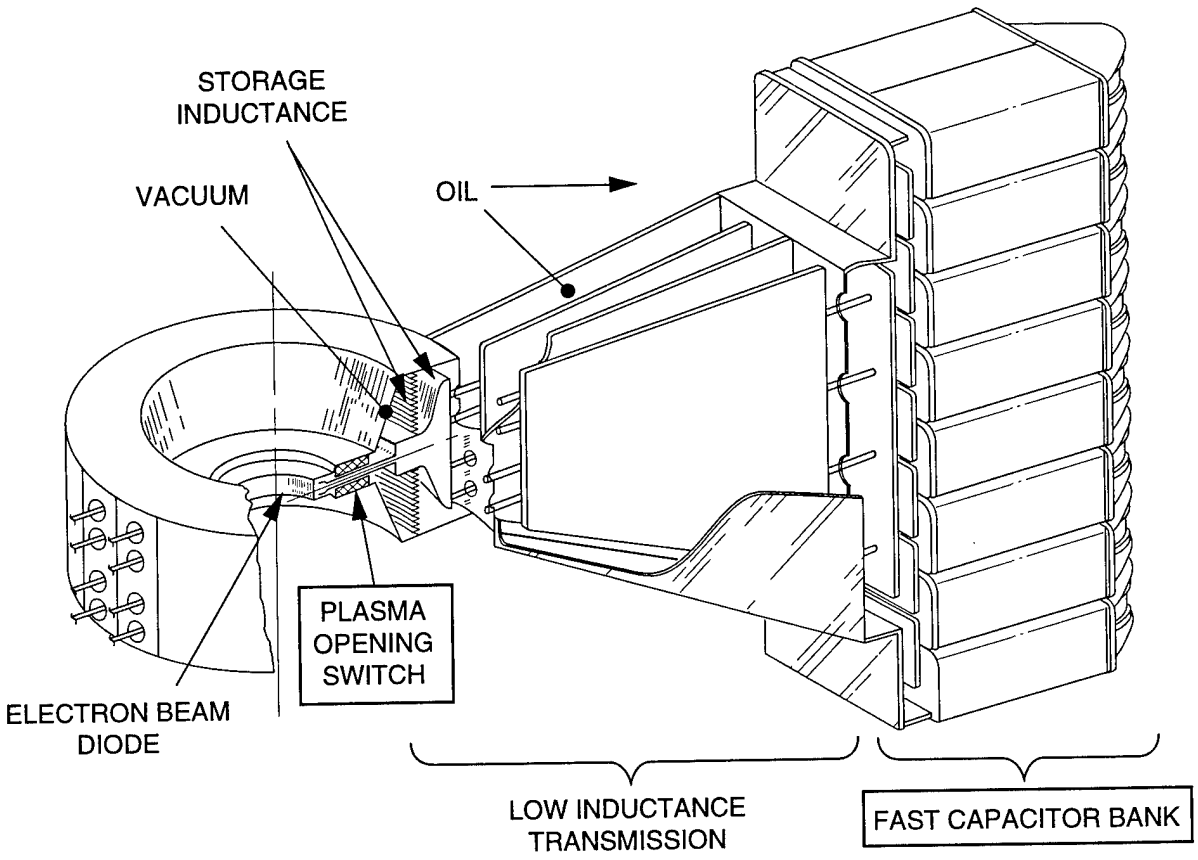

Figure 2-2. ACE 4 cutaway view.

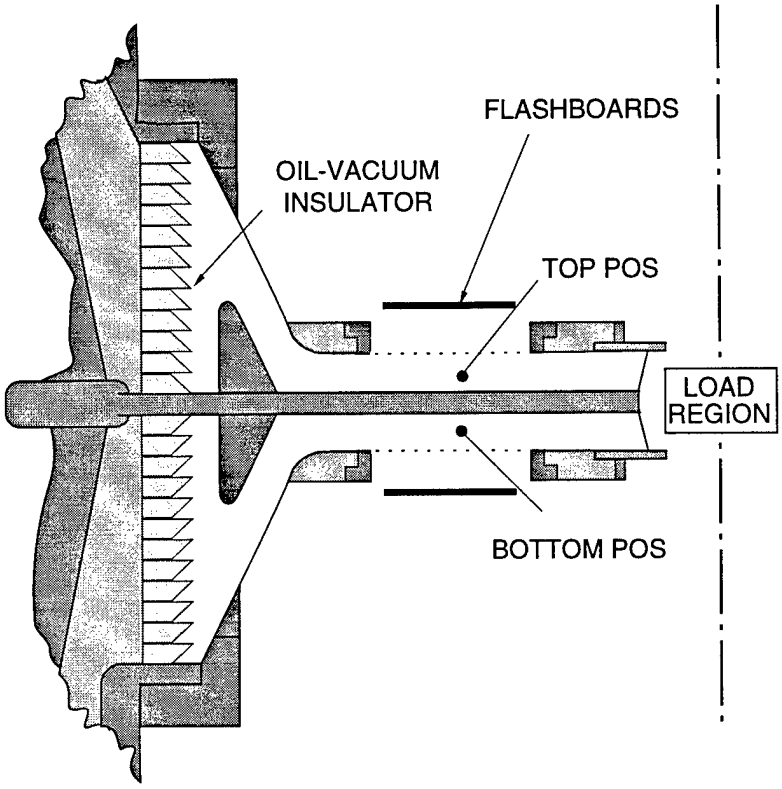

Figure 2-3. ACE 4 radial POS is double sided.

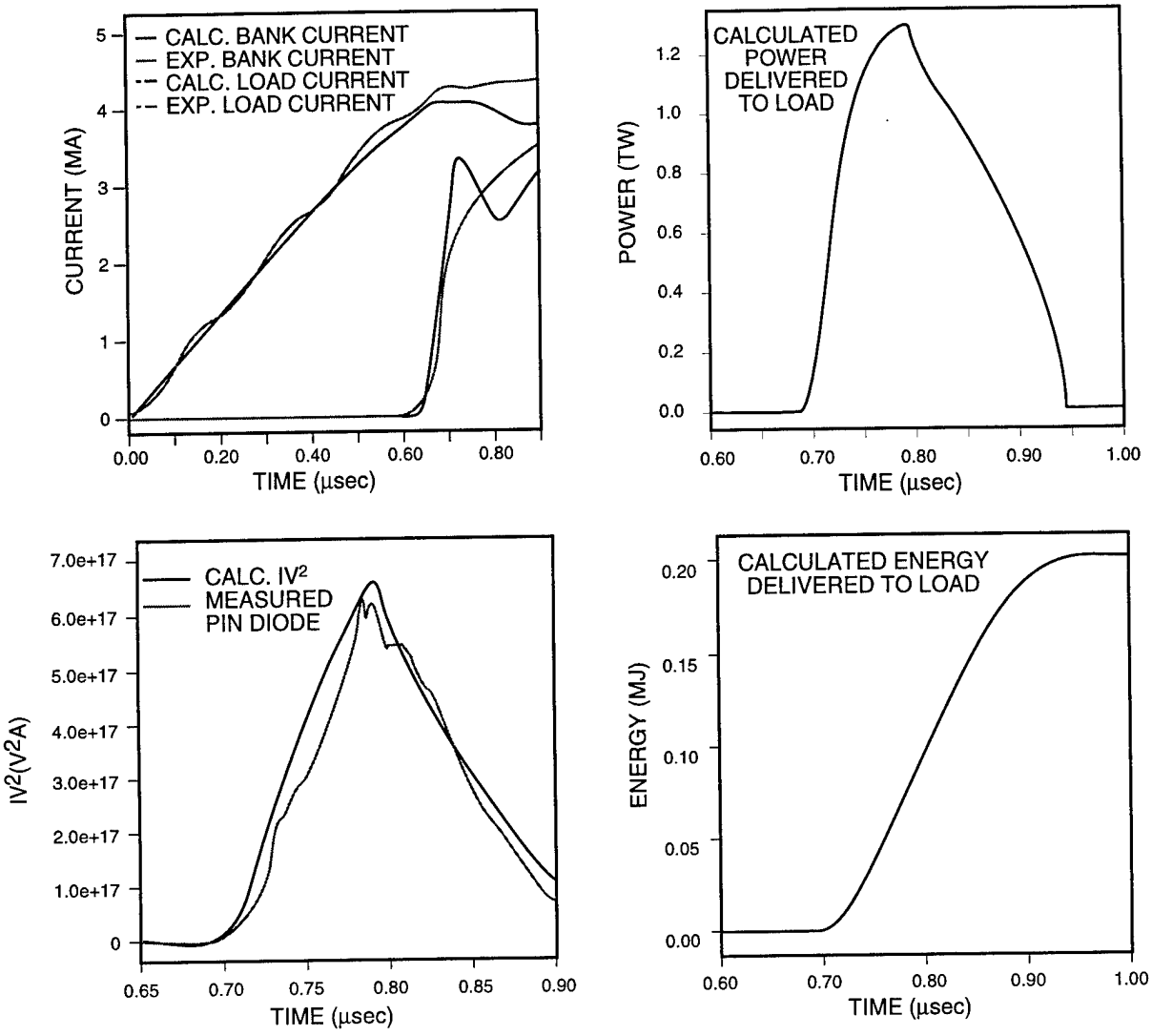

Figure 2-4. ACE 4 performs as expected with unoptimized plasma source.

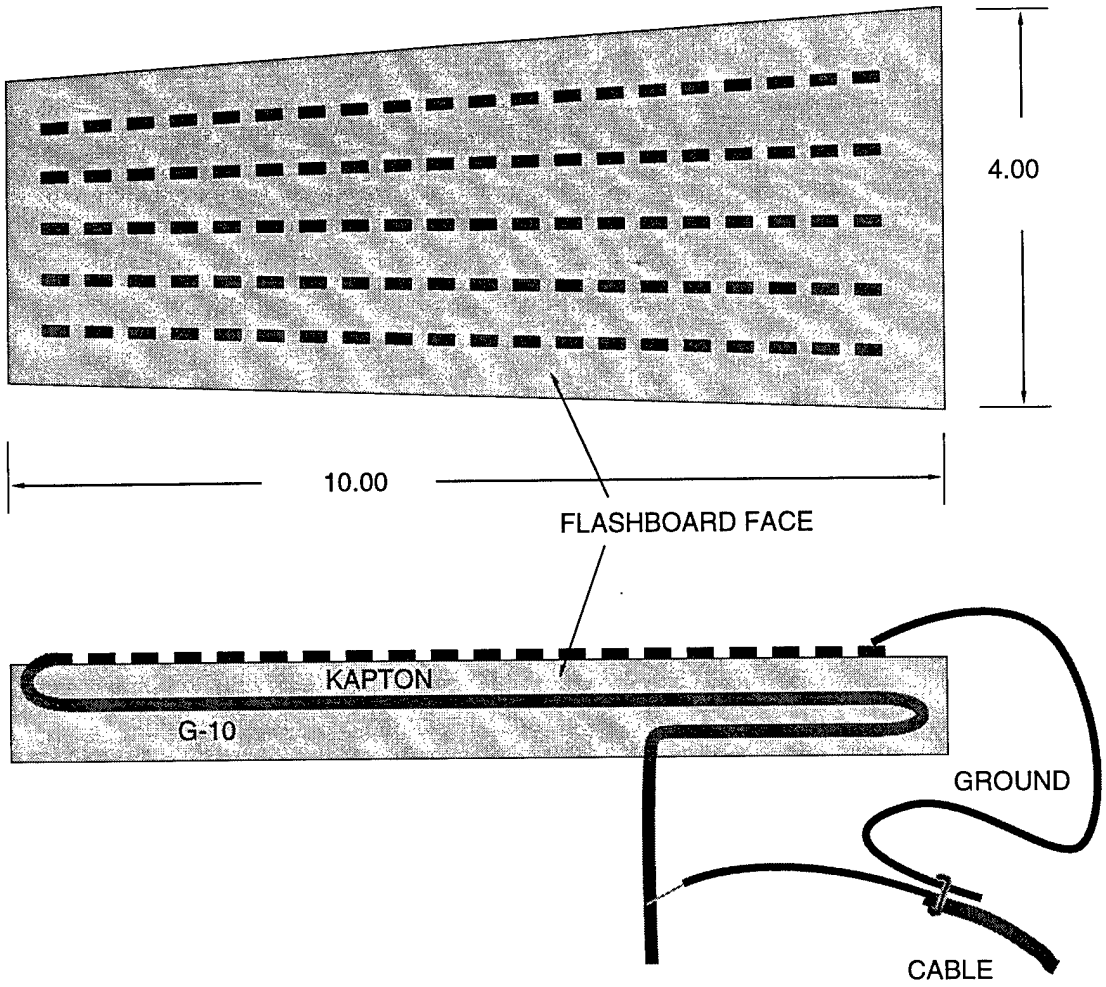

Figure 3-1. Conventional flashboard construction (standard ACE 4).

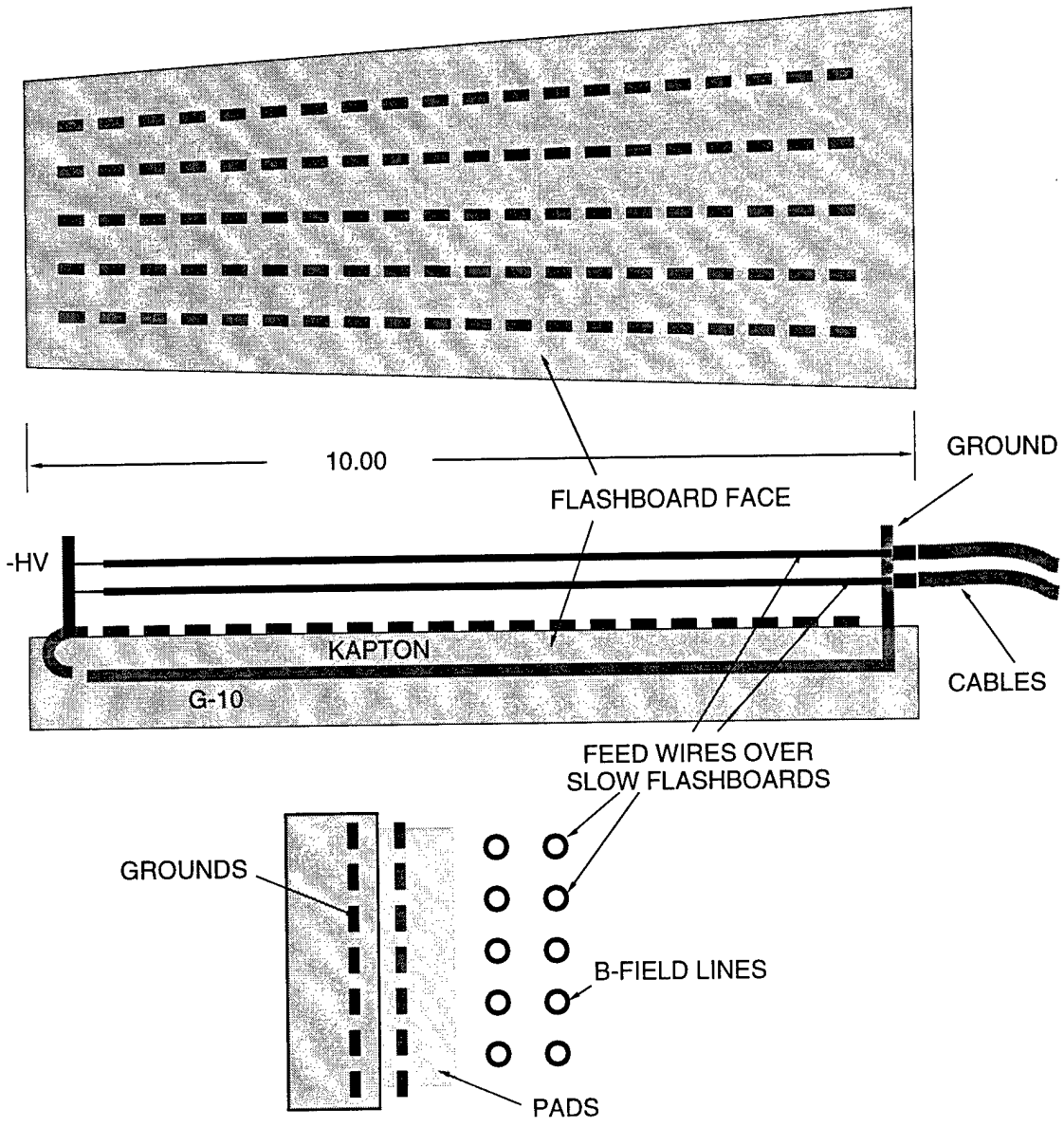

Figure 3-2. Slow flashboard construction.

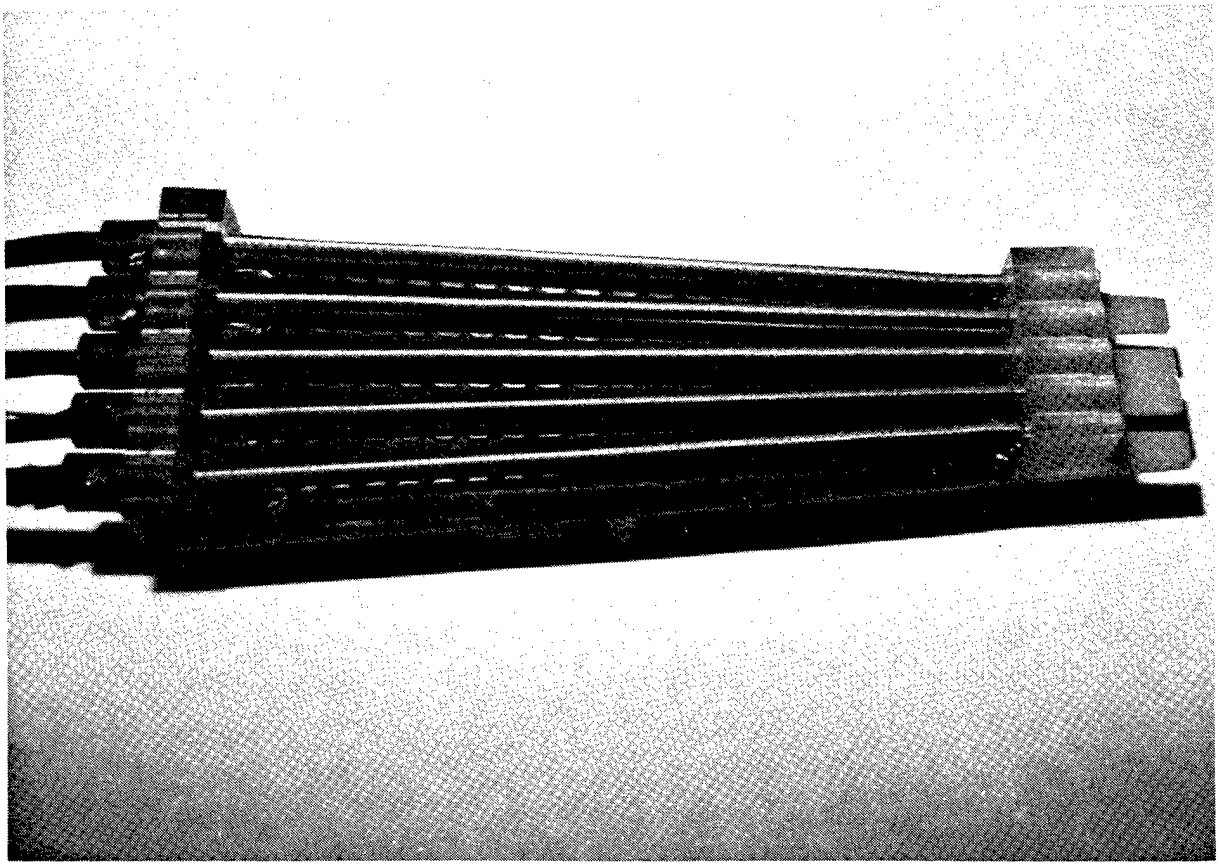

Figure 3-3. A slow flashboard.

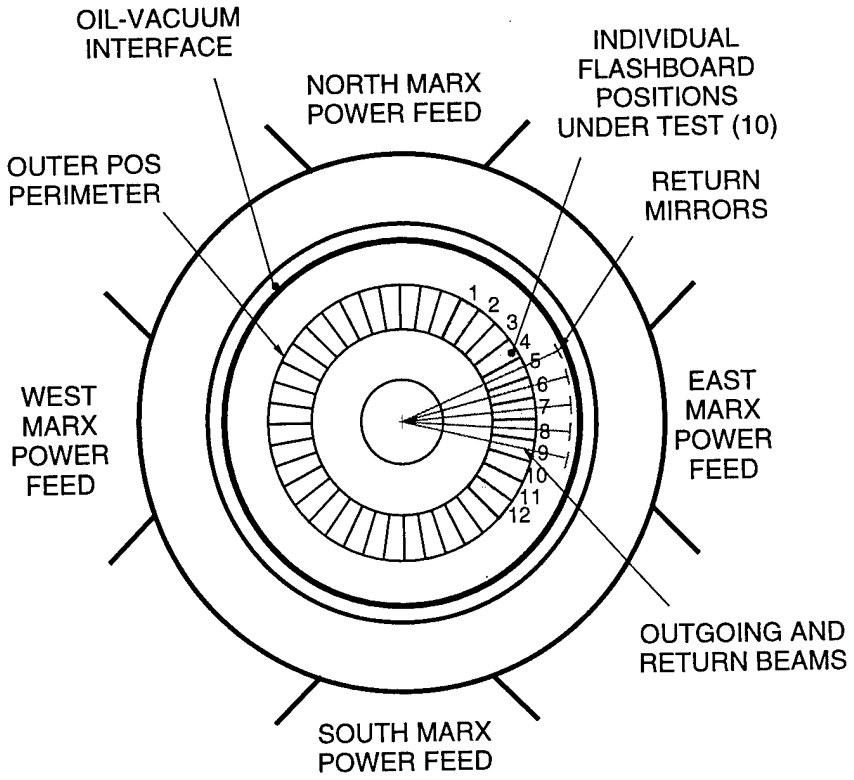

Figure 3-4. ACE 4 old "fast" flashboard characterization configuration.

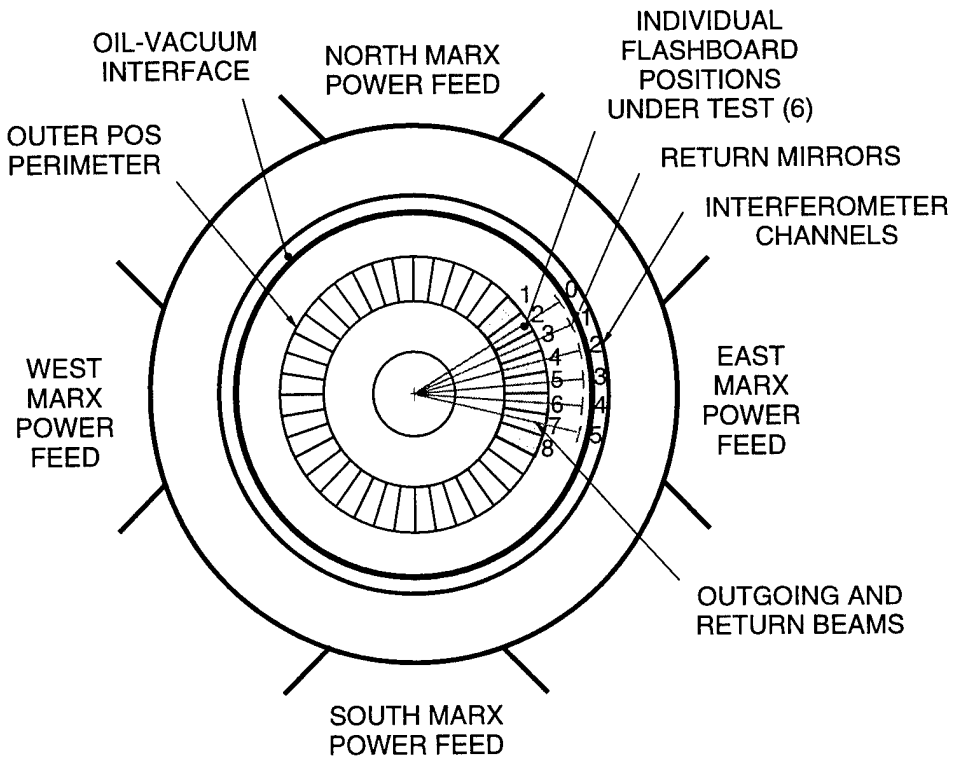

Figure 3-5. ACE 4 new "slow" flashboard acceptance test configuration.

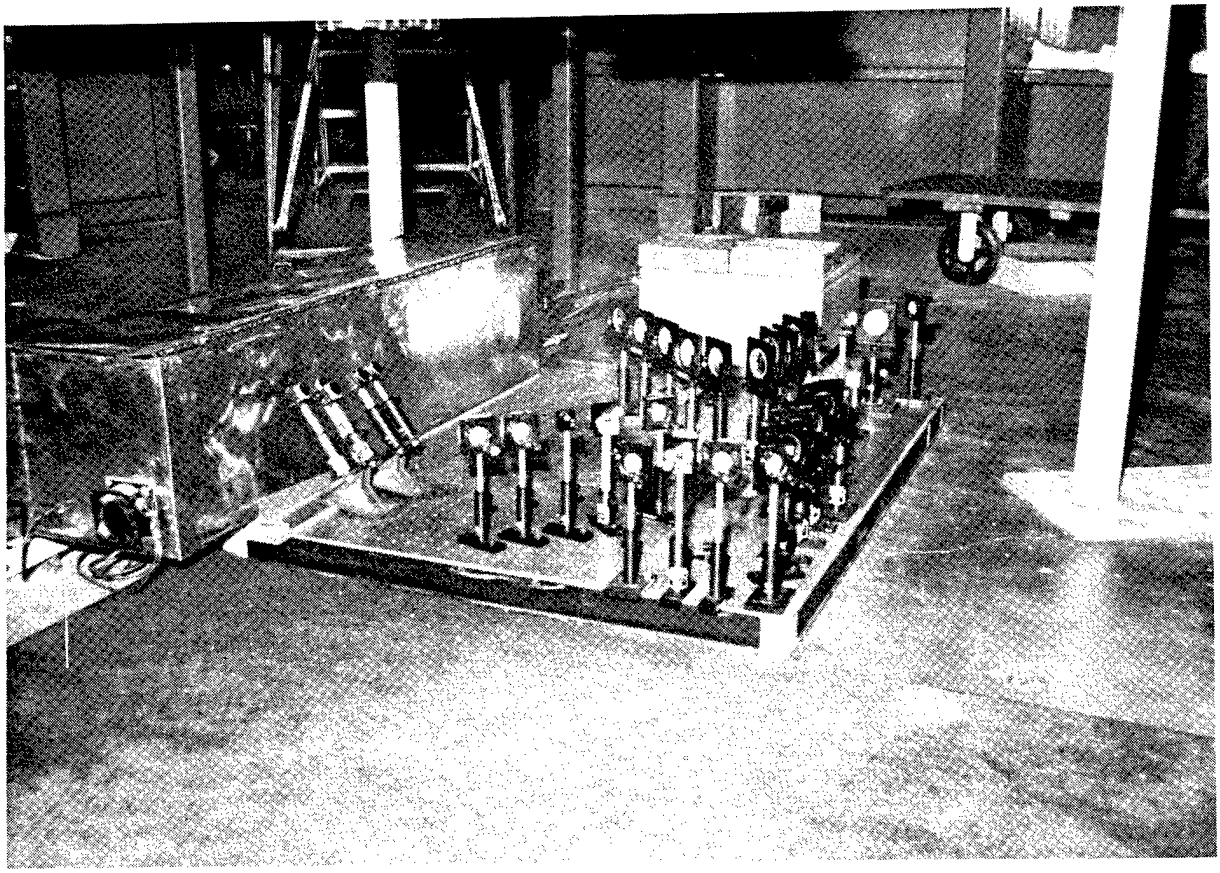

Figure 3-6. Laser and optics used in the 6-channel interferometer.

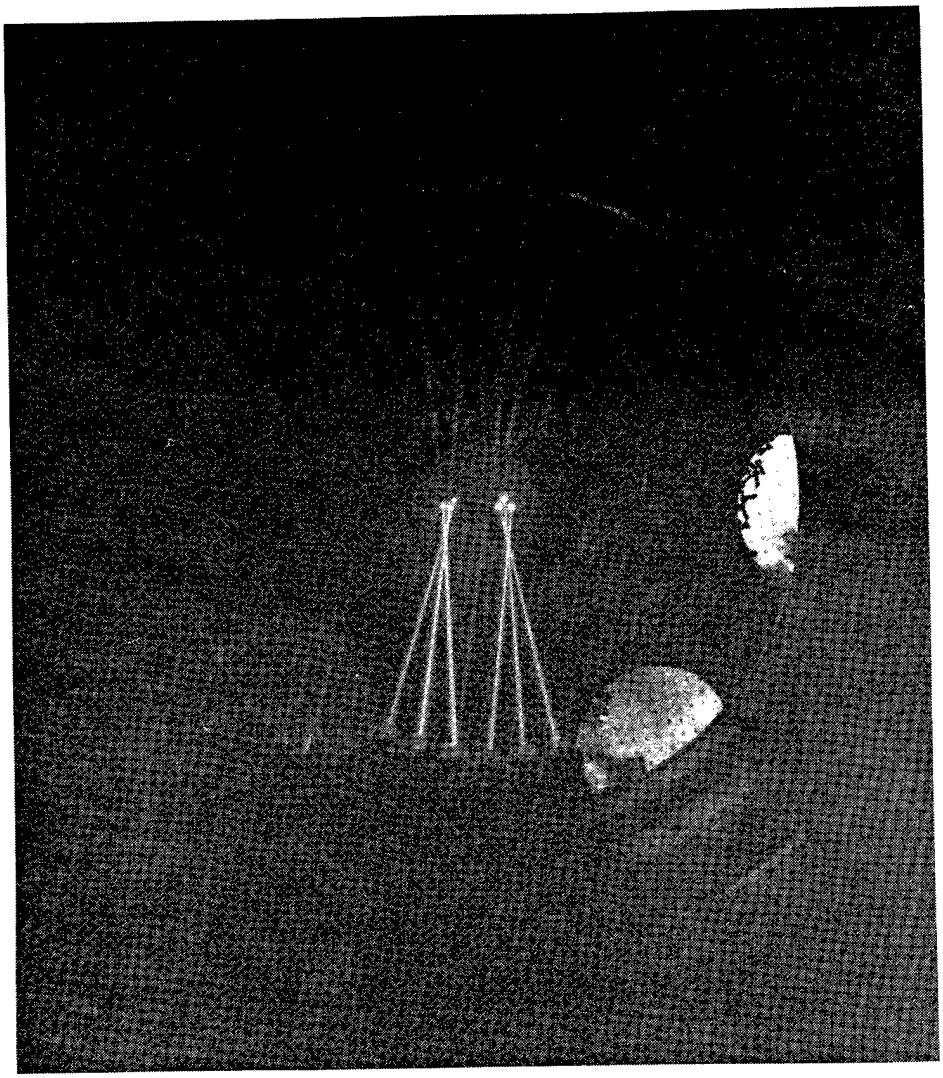

Figure 3-7. HeNe laser beams used in interferometry.

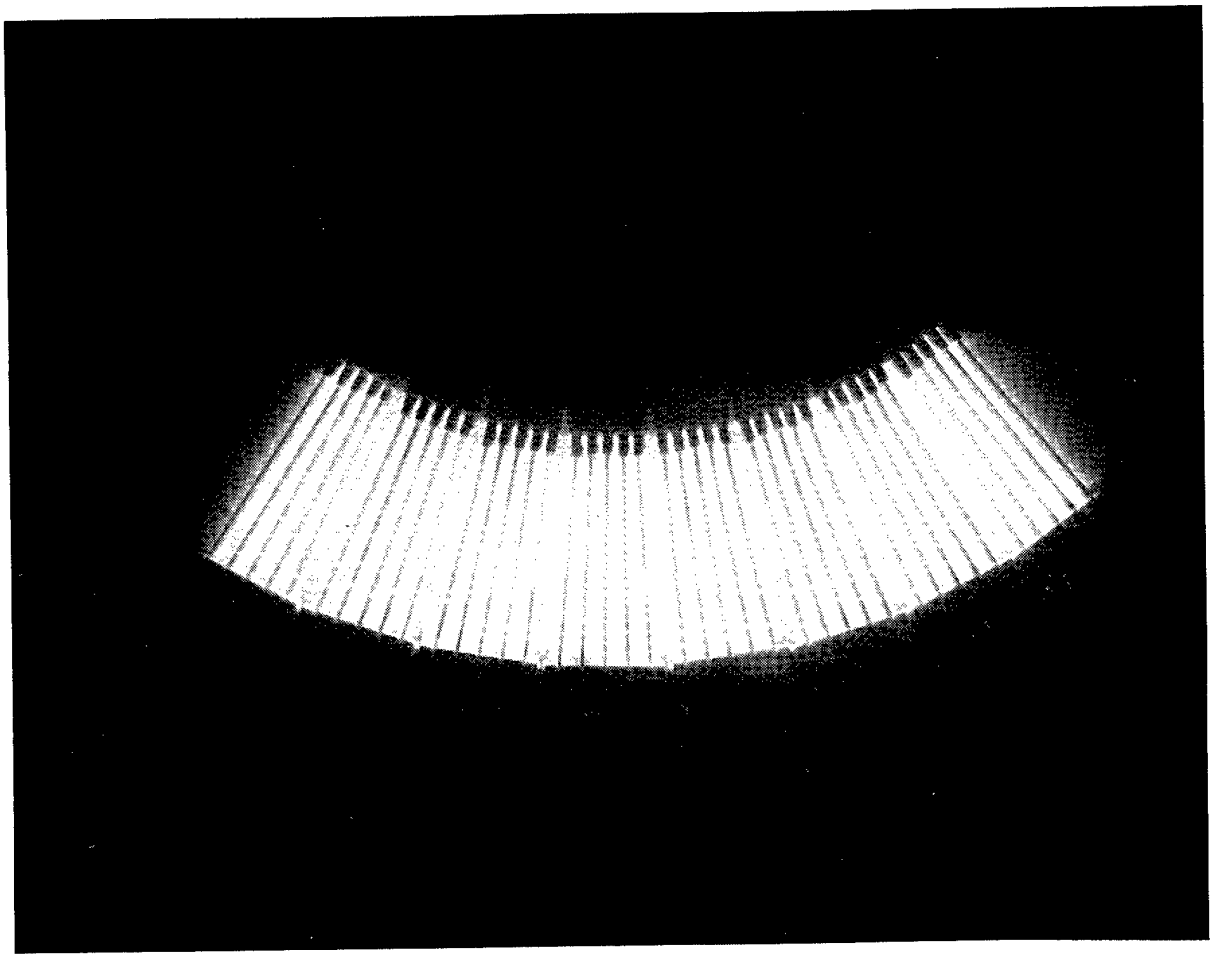

Figure 3-8. Open shutter photograph of slow plasma flashboard array firing.

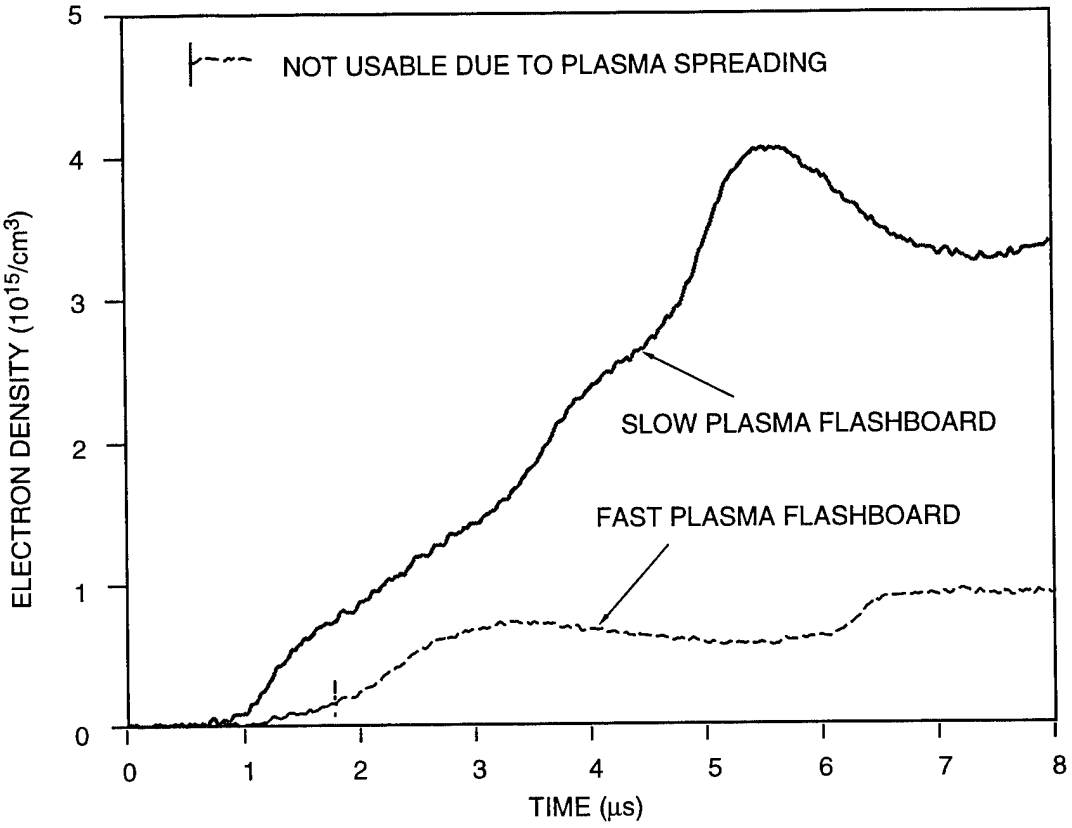

Figure 3-9. Typical density profiles indicate advantages of improved plasma source.

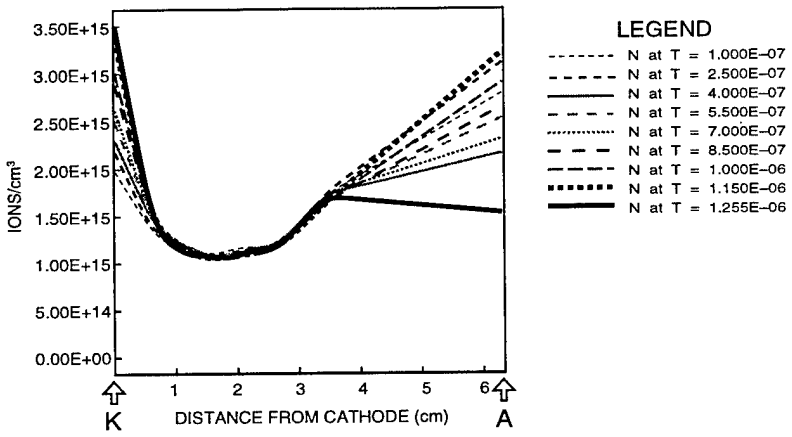

(a) Flashboard density profiles

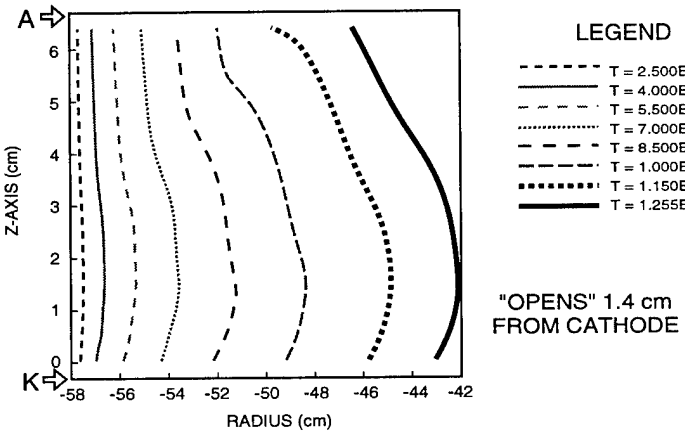

(b) Snowplow fronts

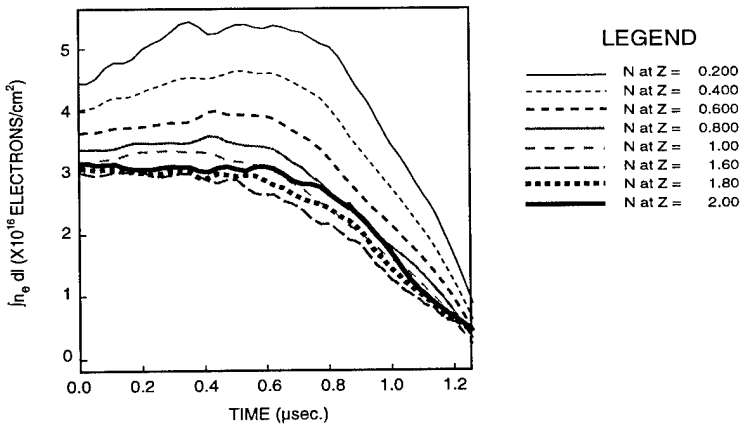

(c) Radial density line integrals

Figure 4-1. Application of snowplow model to ACE 4 shot 821.

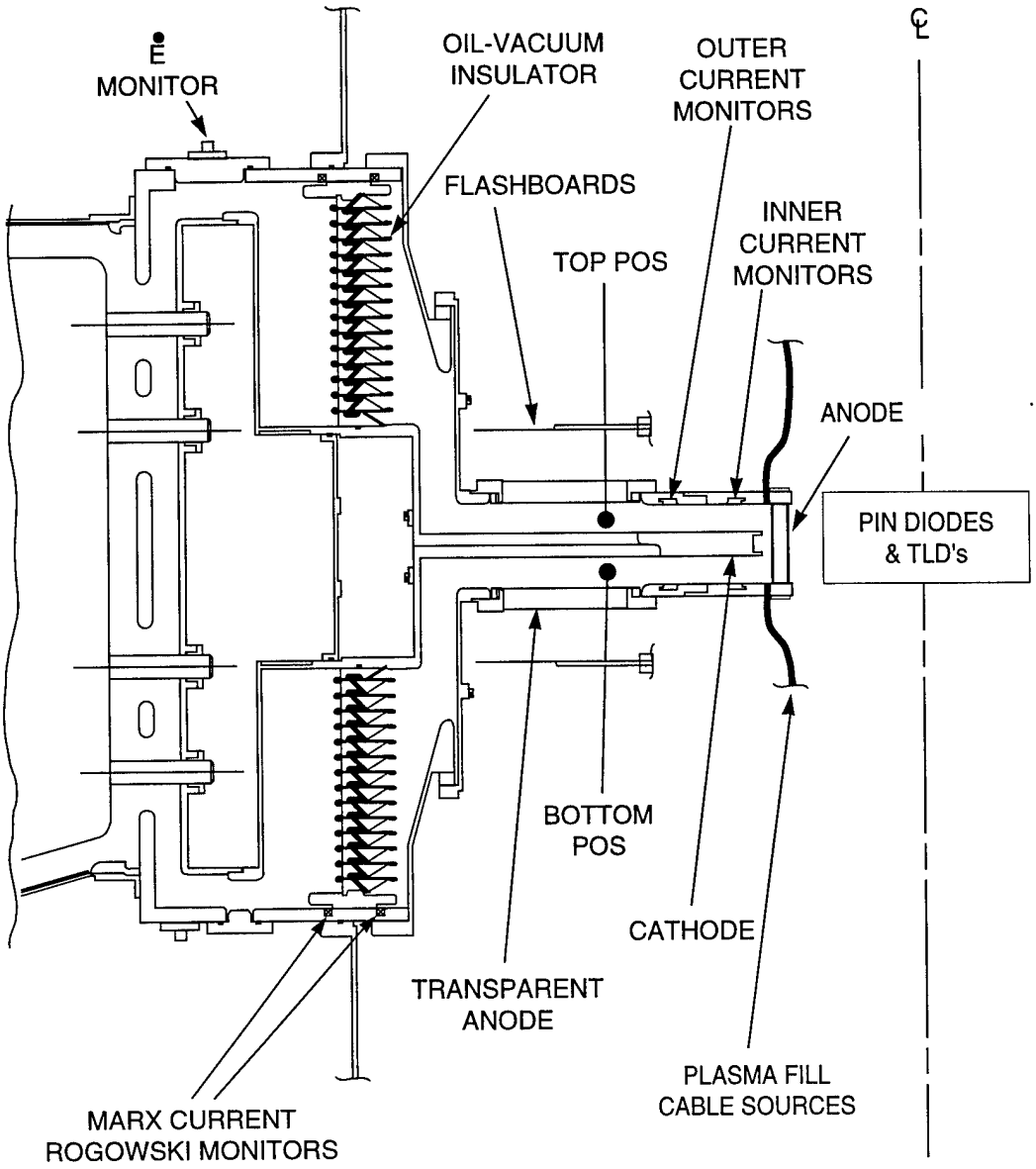

Figure 4-2. ACE 4 radial POS driving an e-beam diode load.

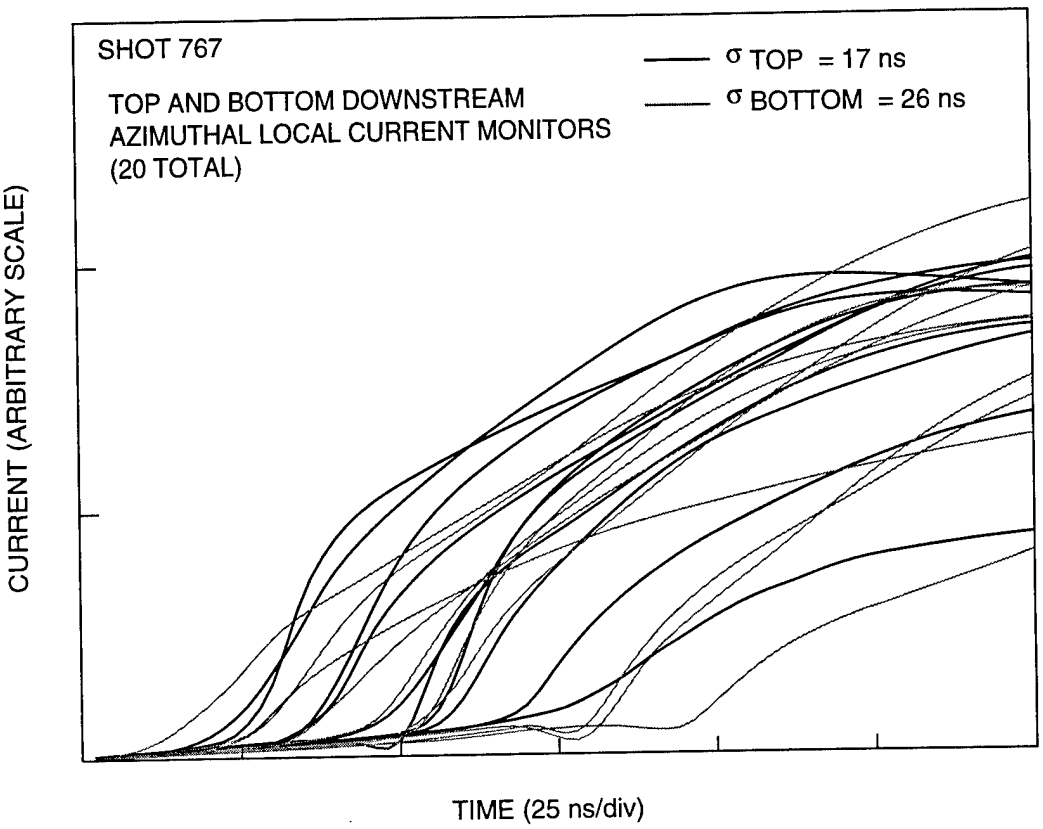

Figure 4-3. ACE 4 POS opening symmetry.

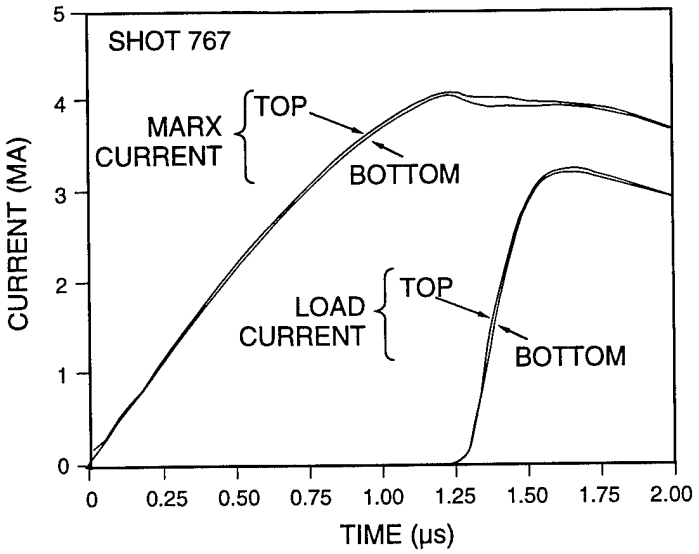

(a) Short circuit load

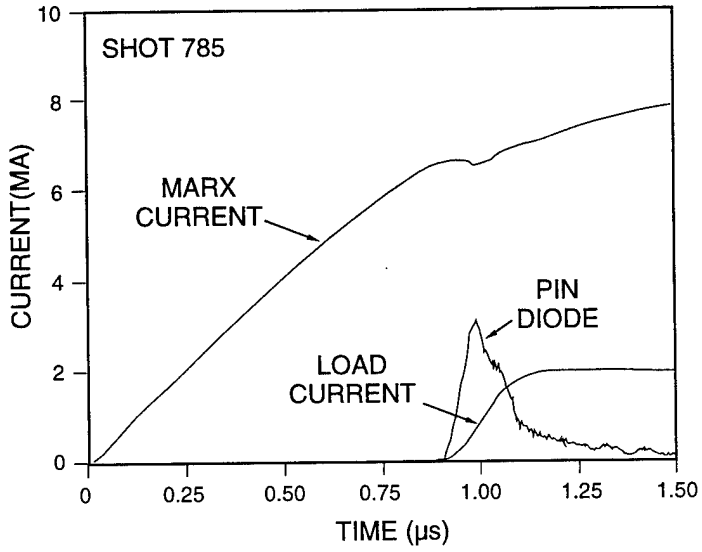

(b) E-beam load

Figure 4-4. ACE 4 POS performance with unoptimized switch plasma distribution.

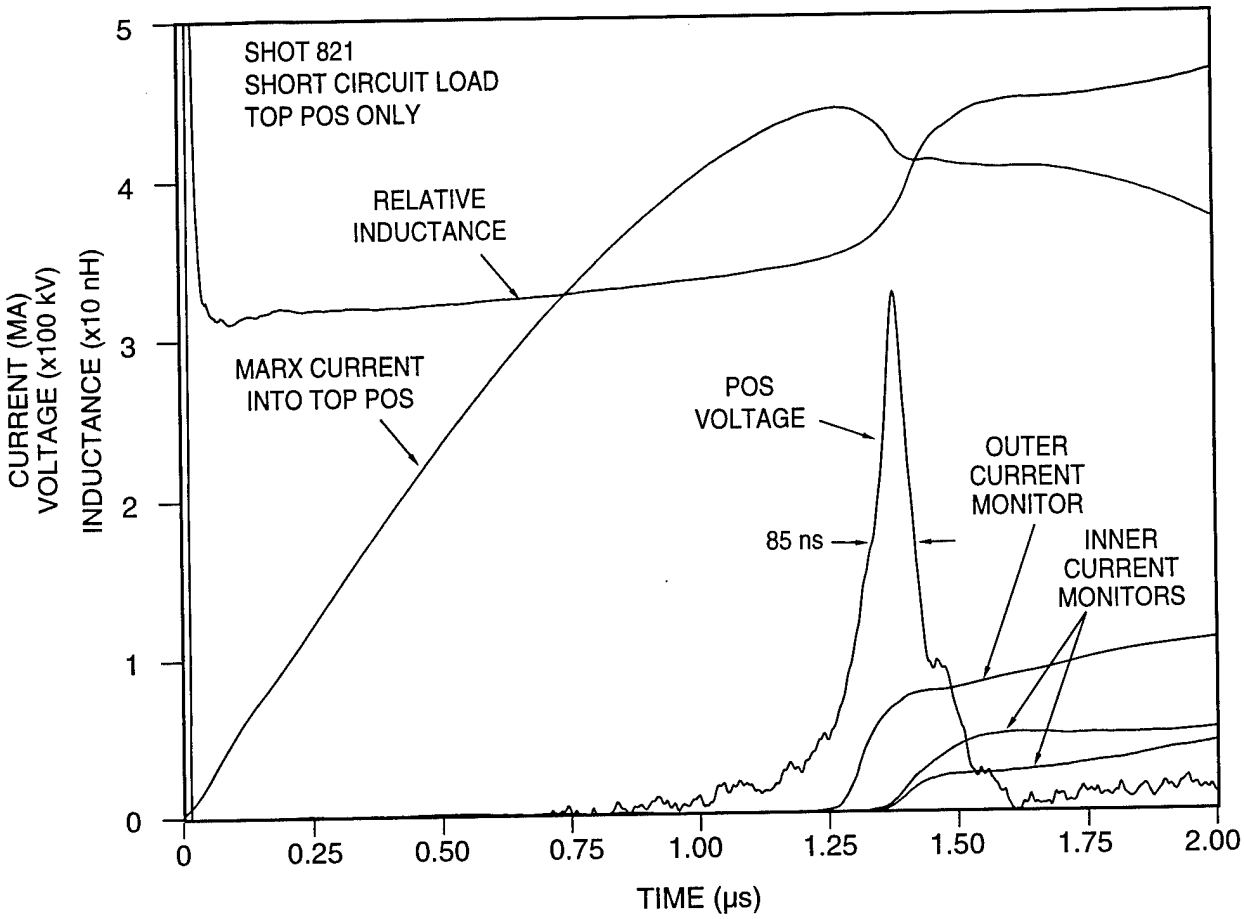

Figure 4-5. ACE 4 POS performance with optimized switch plasma distribution.

DISTRIBUTION LIST

DSWA-TR-95-55

DEPARTMENT OF DEFENSE

DEFENSE SPECIAL WEAPONS AGENCY
ATTN: W SUMMA
ATTN: K WARE
2 CY ATTN: ISST

DEFENSE TECHNICAL INFORMATION CENTER
2 CY ATTN: DTIC/OCP

FIELD COMMAND DEFENSE SPECIAL WEAPONS AGENCY
ATTN: DR BALADI

DEPARTMENT OF THE ARMY

ELECTRONICS TECH & DEVICES LAB
ATTN: PULSE POWER CTR
ATTN: C THORNTON

DEPARTMENT OF THE NAVY

NAVAL POSTGRADUATE SCHOOL
ATTN: F SCHWIRZKE

NAVAL RESEARCH LABORATORY
ATTN: R COMMISSO
ATTN: S OSSAKOW
ATTN: R MEGER
ATTN: G COOPERSTEIN

NAVAL SURFACE WARFARE CENTER
ATTN: CODE B-20

DEPARTMENT OF THE AIR FORCE

AIR FORCE OFFICE OF SCIENTIFIC RSCH
ATTN: DR R BARKER

AIR WEATHER SERVICE MAC
ATTN: AWS TECH LIBRARY

DEPARTMENT OF ENERGY

LOS ALAMOS NATIONAL LABORATORY
ATTN: R REINOVSKY
ATTN: J BROWNELL

SANDIA NATIONAL LABORATORIES
ATTN: J HARRIS
ATTN: J MARTIN
ATTN: M BUTTRAM
ATTN: W BEEZHOLD

OTHER GOVERNMENT

CENTRAL INTELLIGENCE AGENCY
ATTN: J PINA

NASA
ATTN: J LEE

NATIONAL INSTITUTE OF STANDARDS AND TECHNOLOGY
ATTN: R HEBNER

DEPARTMENT OF DEFENSE CONTRACTORS

APPLIED PHYSICAL ELECTRONICS RESEARCH CENTER
ATTN: DR W NUNNALLY

BERKELEY RSCH ASSOCIATES INC
ATTN: R KARES
ATTN: S BRECHT

ENERGY COMPRESSION RESEARCH CORP
ATTN: D S WEIN

FORD MOTOR COMPANY CORPORATION
ATTN: M MOSBROOKER

FORD MOTOR COMPANY CORPORATION
ATTN: C NAKAYAMA

GA TECHNOLOGIES INC
ATTN: DOCUMENT CONTROL

JAYCOR
ATTN: CYRUS P KNOWLES

KAMAN SCIENCES CORP
ATTN: D MOFFETT

KAMAN SCIENCES CORPORATION
ATTN: DASIAC

LORAL VOUTHG SYSTEMS CORP
ATTN: LIBRARY

MAXWELL LABORATORIES INC
2 CY ATTN: E WAISMAN

MAXWELL TECHNOLOGIES INC
2 CY ATTN: D HUSOVSKY
2 CY ATTN: J THOMPSON
2 CY ATTN: R MILLER
2 CY ATTN: W RIX

MINNESOTA MINING
ATTN: D REDMOND
ATTN: E HAMPL

MISSION RESEARCH CORP
ATTN: B GOPLEN

PHYSICS INTERNATIONAL CO
ATTN: C STALLINGS
ATTN: P SINCERNY

PULSE SCIENCES INC
ATTN: P W SPENCE

TETRA CORP
ATTN: W MOENY

TEXAS TECH UNIVERSITY
ATTN: DR M KRISTIANSEN

UNIVERSAL VOLTRONICS CORP
ATTN: W CREWSON

W J SCHAFER ASSOCIATES INC
ATTN: E ALCRAZ

WESTINGHOUSE STC
ATTN: DR A H COOOKSON

OTHER (LIBRARY AND UNIVER)

AUBURN UNIVERSITY
ATTN: M ROSE

UNIVERSITY OF NEW YORK / BUFFALO
ATTN: R DOLLINGER

UNIVERSITY OF CALIFORNIA / DAVIS
ATTN: J S DEGROOT